scientific reports

Check for updates

OPEN

Enhanced horizontal deposition of large stone in granular flow with mixing small spherical grains after slide along slope and free fall

Hai-Hua Gu[1]✉, Lin-Tao Fu[2] & Yu Lei[1,3]

Geophysical mass flows, which could endanger our health, lives, and property safety, commonly occur in mountain regions. Although many efforts have been made, transport of granular flows consisting of polydisperse grains, which is influenced by multiple factors, is still not well understood. This work focused on the effect of small spherical grains on the movement of large stones in granular flows of different grain compositions (quartz gravel, glass bead and angular stone), through experimentally measuring mass frequency distributions of granular materials deposited on flat surface. Three characteristic deposition distances (X_{20}, X_{50} and X_{80}) and one extreme mobility probability (P_s) were extracted from cumulative frequency distributions. It reveals that, in most of cases, the inclusion of glass beads reduced X_{20}, X_{50}, and X_{80} but increased P_s for total mass. For angular stone mass, the inclusion of glass beads increased the occurrence frequency of that X_{20}, X_{50} and X_{80} increase, apart from increasing P_s. These results indicated small spherical grains could effectively enhance the extreme mobility of large angular stones in mixtures. We hope these results could be helpful for improving our understanding of the transport of geophysical mass flow as well as the grain segregation in different natural environment.

Keywords Extreme mobility, Grain segregation, Grain composition, Grain sphericity, Mass distribution

Granular materials are important components of Earth system. The transport of granular materials, the sizes of which range from 10^{-6} m (e.g., dust particles) to 10^{2} m (e.g., large falling rock), widely occurs in both natural environment and engineering environment (include landslides, debris flows, flash floods, sand storm and so on), and commonly endanger our health, lives, and property safety. For instance, severe sand and dust storm (in which extremely high grain concentration sharply decreased air visibility and air quality) in Northwest China on 1993/05/05 disrupted railways and caused the delay or cancellations of both trains and flights[1]. The landslides, rockfalls, and debris flows, which contained granular materials of different sizes and were induced by the 2008 Wenchuan earthquake in Sichuan Province, China, killed about 20,000 lives[2]. Therefore, investigations on the transport of granular materials are not only attracting the attention of scientists but also important for engineers who are making their efforts to prevent or reduce the disaster risks in field.

Granular materials both in nature and in industry are typically polydisperse[3,4], which would lead to grain segregation because of differences in grain motions[5–8]. To better understand geophysical mass flows, such as landslides, rockfalls, and debris flows, grain segregation has been investigated for a long time through different methods[9–14]. Laboratory investigations[6,15–21] and field observations[22–24] suggested that grain segregation mechanisms were diverse and affected by multiple factors.

For example, the grain size of granular mixtures played a very important role in grain segregation[25] and the transport of grain flow[26]. Including large particles into small (original) particles or increasing grain size ratio between large particles and small particles, which would alter the grain composition (or grain size distribution), could enhance the transport distance of released granular materials in laboratory experiments[15,27]. Discrete Element Method (DEM) simulations have been used to show that the inclusion of fine particles has been shown to enhance flow speed in bidis perse mixtures[28,29]. Field observations on landslide deposits also revealed that large grains appeared to move further compared to small grains[23]. Besides, grain shape (particularly for grain sphericity) was another important factor contributing to grain segregation and grain transport[4]. Laboratory

[1]Institute of Mountain Hazards and Environment, Chinese Academy of Sciences (CAS), Chengdu 610041, China. [2]School of Architecture and Civil Engineering, Chengdu University, Chengdu 610106, China. [3]China-Pakistan Joint Research Center on Earth Sciences, CAS-HEC, Islamabad 45320, Pakistan. ✉email: guhaihua@imde.ac.cn

experiments suggested that the degree of grain segregation could be enhanced with increasing grain sphericity[30]. Recent experimental investigation on the resultant deposition patterns of 16 repeats in each case revealed that the degree of grain segregation increases with the absolute values of relative size factor and relative shape factor, and relatively large and rounded particles would be transported further[31].

Generally speaking, many efforts as mentioned above have been made to improve our understanding of geophysical mass flows; however, there are some aspects of disadvantages, which would limit our understanding of the transport of granular materials as well as large particles, particularly for some specific cases in nature. One of such cases is that granular materials are originated from the top region of a hill in mountain area and a height drop existed between the lowest point of hill slope and the foot of hill[32]. Buildings or roads are usually constructed not at the foot of the mountain slope but like we shown in the Fig. 1 below. The granular matters falling from the slope (debris flows, rolling stone and fall rack) may impact on the building on the ground or the vehicles on the road. In fact, such disaster frequently occurs in mountain area in China. The granular materials would thus experience three different stages under sufficiently external excitation. These stages include initial slide along hill slope, subsequent free fall from the end of slope to the foot of hill, and final horizontal movement along local terrain at the foot of hill. Most of previous experiments usually involved two of the three stages, which leads to incompletely interpret field observations in such case. Besides, extreme mobility (or long runout) of geophysical mass flows[33,34] is an interesting but puzzling phenomenon, which is still not well-understood so far. Although field observations revealed that the circularity of small grains in rockslide-debris avalanches remarkably increased with the distance from source location[33]. However, less attention has been given to the influence of small rounded grains, particularly their proportion in granular mixtures, on the transport of large angular grains.

Therefore, this piece of work experimentally investigated how deposition characteristics (four characteristic quantities derived from cumulative frequency distributions of deposited mass) of both total granular materials and large angular stone change with the fraction of small round grains, when the granular materials initially slid along a slope, then experienced free fall, and finally moved on a flatbed surface. Three types of grain compositions were designed. The first type, serving as a reference for the other two, included only small angular grains and large angular stones, with variations in their mass fractions. The second type maintained a 1:1 mass ratio of angular stones to round small grains, while varying the mass fraction of small angular grains in the total granular mixture. The final type maintained the mass fraction of small angular grains at 60% of the total granular mixture, while varying the mass ratio of angular stones to round small grains. In the following, experimental design and data processes were described in details, both qualitative and quantitative results were then briefly shown, and finally concise discussion were presented.

Materials and methods

Experimental equipment

Experiments were conducted at Key Laboratory of Mountain Hazards and Earth Surface Processes, Chinese Academy of Sciences, Chengdu, China. Experimental equipment mainly consisted of two parts, a chute and a horizontally open channel, as shown in Fig. 1. The size of chute was 0.5 m (inner width) × 2 m (length) and the size of open channel was 0.6 m (inner width) × 2 m (length). Both beds and sidewalls of the chute and the open channel are made of toughened glass. So, the bed surface is very flat and less frictional in comparison to natural land surface.

The open channel was not laid on the floor but fixed at the location of 25 cm height above ground. In contrast, the chute was supported by the table which was fixed on the floor and is 0.97 m in height. The chute did not fully cover on the table but had an overhang of 0.7 m (right hand from the view of Fig. 2) to make experiments done smoothly. In indoor laboratory experiments and numerical simulations, a wide range of the inclination angle (10°–60°) was selected for the chute[35–41] and the inclination angle of 35°–45° was frequently used. Thus, the slope (θ) of the chute was set as 40° during all experiment runs in this paper. So, there is a 0.27 m drop in height between the lowest point of the chute and the bed of open channel.

A wood block (the solid red line in Fig. 2b), which is 0.6 m in length (not the direction perpendicular to chute bed but the direction parallel to chute width) and 0.02 m in thickness, was semi-fixed at the location 0.5 m from the left endpoint of the chute (i.e., the opposite endpoint relative to the overhang). A hopper, which was used to store granular materials, was formed by chute bed, chute sidewall and wood block. During each run,

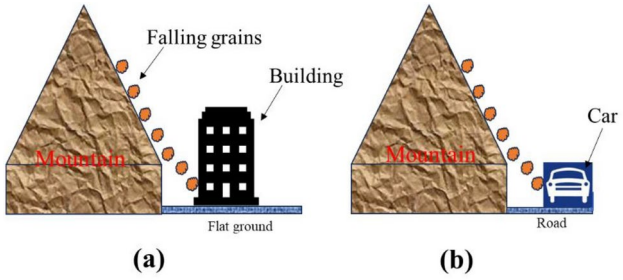

Fig. 1. Schematic diagram of the buildings or roads at the foot of the mountain slope.

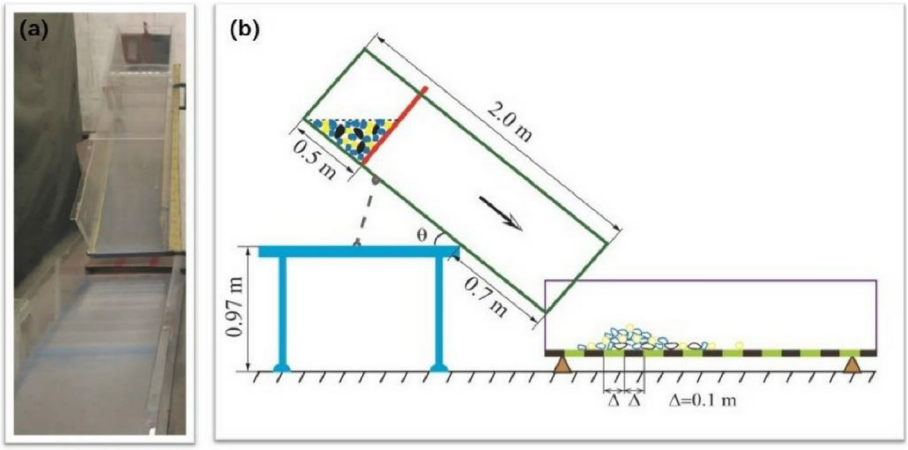

Fig. 2. Experimental equipment and schematic diagram of experiment. Grains (open) on open channel surface suggest a possible deposition pattern of grains (solid) released from storage hopper.

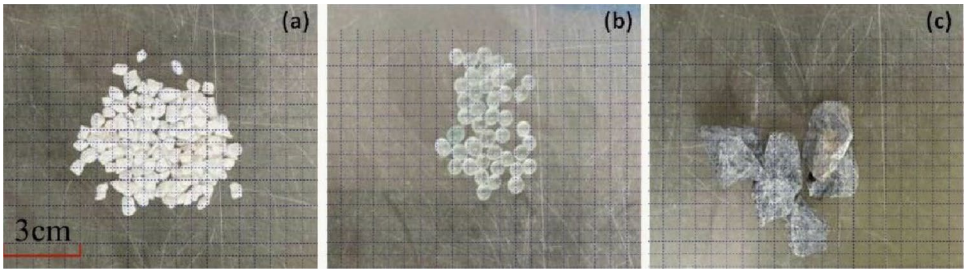

Fig. 3. Granular materials used in experiments. (**a**) Quartz gravel, (**b**) glass bead, and (**c**) angular stone.

granular materials in the hopper were released through quickly pulling the wood block out along the direction perpendicular to chute bed.

Granular materials

In this study, three types of grains, quartz gravel (QG), glass bead (GB) and angular stone (AS), were employed, as shown in Fig. 3. Quartz gravel is typically angular. The size of quartz gravel ranges from 5 to 13 mm, with an average value of around 8 mm. Glass bead is highly spherical. The size of glass beads ranges from 6 to 7 mm, with an average value of around 6.5 mm. Angular stone is significantly larger than both quartz gravel and glass bead. The size of angular stones ranges from 19 to 39 mm, with an average value of around 26 mm. The densities of quartz gravel, glass bead and angular stone are about 2300 kg/m^3, 2700 kg/m^3 and 2900 kg/m^3, respectively.

In each run, total weight of granular materials was around 5 kg (relative fluctuation was smaller than 2%). In most previous studies (both experiments and simulations), the total mass of dry granular materials is large enough to form a thick grain layer. Thus, the segregation mechanisms under ideal conditions could be well explained. Therefore, our results obtained bases on the total mass of 5 kg could only be partially explained by the findings from ideal conditions. Nevertheless, it reminds that, the disaster of dry granular particles under natural conditions in mountain area is diverse, and the source of dry granular materials on the slope of potential disaster may be thin like our experiments. The findings from ideal conditions cannot be always applied, while our experimental results may provide empirical/specific insights. Weight fluctuations during experiment preparation usually occurred when angular stones were used, due to the significant weight of each stone. Besides, total weight of granular materials collected after sliding and falling was typically smaller than the originally released weight. Due to their angular edges, quartz gravel particles easily broke into small, dusty grains upon colliding with the bed of the horizontal channel and other angular stones.

Based on the aim of this work, 15 cases of grain compositions for granular materials in terms of weight percentage were designed. These cases (ordered by the weight percentage of quartz gravel) were (1) QG 100%, AS 0%, GB 0%, (2) QG 80%, AS 20%, GB 0%, (3) QG 80%, AS 10%, GB 10%, (4) QG 70%, AS 30%, GB 0%, (5) QG 70%, AS 15%, GB 15%, (6) QG 60%, AS 40%, GB 0%, (7) QG 60%, AS 30%, GB 10%, (8) QG 60%, AS 20%, GB 20%, (9) QG 60%, AS 10%, GB 30%, (10) QG 60%, AS 0%, GB 40%, (11) QG 50%, AS 50%, GB 0%, (12) QG 50%, AS 25%, GB 25%, (13) QG 40%, AS 60%, GB 0%, (14) QG 40%, AS 30%, GB 30%, and (15) QG 0%, AS 100%, GB 0%.

Experimental procedures

During each run, granular materials were firstly stored in the fixed hopper mentioned above after weighting. In cases that granular materials were consisted of more than one kind of grain compositions, simple stirring and shaking of granular materials in a plastic bucket (0.6 m in height and 0.35 m in diameter) were employed to make a roughly homogeneous distribution of different grains. Then, the uneven surface of stored materials was manually flattened to horizontally parallel the ground surface as well as the open channel bed. Thirdly, the wood block was quickly pulled out along the direction perpendicular to the chute bed, and granular materials finally deposited on the open channel bed after sliding along the chute and freely falling. Fourthly, the deposited materials were gathered along fixed intervals in proper order. The width of each interval (i.e., Δ in Fig. 2b) is 0.1 m. The intervals were marked by marker pen at both bed and sidewalls of open channel before experimental runs. More than 16 intervals were involved from the left end of open channel to the right end; and the materials deposited farther than 1.5 m from the left end were all gathered in the 16th interval because the materials deposited in this region accounted for very small fraction. Finally, the granular materials gathered in each interval were weighed and recorded for further analyses. In this step, two sub-steps were applied when granular materials contained angular stone. The first sub-step was weighing the mass of all granular materials in an interval, and the second one was weighting the mass of angular stone (Angular stone is easily separated from the mixture, because it is significantly larger than other two types of grains). To reduce the uncertainties caused by unexpected or undetected reasons, five runs were repeated for each case.

Data processes

As mentioned above, there are total 16 data points (namely 16 weight data) in a run for a specific case. The central locations (X_{ci}, $i \in [1, 16]$) of each interval from the 1st interval to the 16th interval are 5 cm, 15 cm, 25 cm, 35 cm, 45 cm, 55 cm, 65 cm, 75 cm, 85 cm, 95 cm, 105 cm, 115 cm, 125 cm, 135 cm, 145 cm, and 155 cm, respectively. And, the node locations (X_{ni}, $i \in [1, 17]$) of each interval from the 1st interval to the 16th interval are 0 cm, 10 cm, 20 cm, 30 cm, 40 cm, 50 cm, 60 cm, 70 cm, 80 cm, 90 cm, 100 cm, 110 cm, 120 cm, 130 cm, 140 cm, 150 cm, and 160 cm, respectively. Let the weight of granular materials in an interval be denoted as w_i, the total mass of all intervals is then determined as $\mathrm{w} = \sum_{\mathrm{i}=1}^{16} \mathrm{w_i}$. The mass frequency f_i of granular materials in an interval is determined as $f_i = w_i/w$, and the cumulative mass frequency f_i of granular materials along with the increase of intervals is determined as $F_{i+1} = F_i + f_i$ (Here, $i \in [1, 16]$, $F_1 = 0$ at $X_{n1} = 0$ cm, and $F_{17} = 1.0$ at $X_{n17} = 160$ cm).

To better understand the differences in mass distributions among different cases, four characteristic quantities, X_{20}, X_{50}, X_{80}, and P_s, were employed. X_{20}, X_{50}, and X_{80} are the distances at which cumulative frequency reaches 20%, 50%, and 80%, respectively. X_{20}, X_{50}, and X_{80} were used to reflect the short distance transport, median distance transport, and long-distance transport of granular materials, respectively. P_s (called 'extreme mobility probability') was used to reflect the extreme long-distance transport of granular materials. The value of P_s here is set to equal the mass frequency of granular materials in the 16th interval (i.e., f_{16}). In contrast, the values of X_{20}, X_{50}, and X_{80} were usually obtained through simple linear interpolation, because those specific cumulative frequencies most of time would not be just right reached at either node location of an interval. If a specific cumulative frequency F (i.e., 20%, 50% and 80%) falls within the ith interval, the linear interpolation for the corresponding characteristic distance X is shown as Eq. (1).

$$X = \left[F\left(X_{ni+1} - X_{ni}\right) - \left(F_i X_{ni+1} - F_{i+1} X_{ni}\right)\right] / \left(F_{i+1} - F_i\right). \tag{1}$$

Because there were five runs for each case, the mean value and standard deviation (S.D.) for every quantity were calculated. Suppose the value of a specific quantity in a run as Y_k, the mean value of this quantity among five runs was calculated as $\mathrm{Y} = \sum_{\mathrm{k}=1}^{5} \mathrm{Y_k}/5$, and the corresponding standard deviation was calculated as $S.D. = \sqrt{\sum_{K=1}^{5} \left(Y_K - Y\right)^2/4}$. Origin software[42] was employed to conduct quantitative analyses and curve fits for raw data if necessary.

Tables 1 and 2 shows the means and standard deviations (S.D.) of the four characteristic quantities, X_{20}, X_{50}, X_{80}, and P_s of 15 cases of grain compositions for granular materials in terms of weight percentage in our experiment.

Results

The motion of granular particles along the chute (a camera was installed at the lowest end of the chute) of 2 cases of grain compositions for granular materials in terms of weight percentage (case7-QG 60%, AS 30%, GB 10% and case-10) QG 60%, AS 0%, GB 40%) were show in Fig. 4, the video is also available as supplementary material. We can find that the angular stone (which are large 19 to 39 mm) are not bouncing down the chute but are moving as a coherent avalanching body with quartz gravel and glass bead along the chute from the video. Consequently, the angular stones, most of time, lay on the smaller grains (glass beads and quartz gravels), with a low chance to contact the chute bed. Of course, one possible reason for the non-bounce of the angular stones is the flat and low friction chute bed. Besides, the stream-wise distribution of large angular stones in the coherent avalanching body in cases of with no glass beads is more homogeneous than that in cases of with glass beads, when they are moving along the chute bed.

In this section, the deposition characteristics of granular materials on the open channel bed after sliding along the chute and freely falling among different cases were compared in two ways. The first way was qualitative comparisons of the cumulative frequency distributions of granular mass among different cases, and the second one was quantitative comparisons of the four characteristic quantities among different cases.

Grain compositions in cases				X_{20} (cm)		X_{50} (cm)		X_{80} (cm)		P_s	
				Mean	S.D.	Mean	S.D.	Mean	S.D.	Mean	S.D.
1	QG100%	AS0%	GB 0%	59.6	1.4	70.5	2.0	82.5	2.5	0.0163	0.000743
2	QG80%	AS20%	GB 0%	57.2	2.1	68.9	2.0	82.8	2.6	0.0232	0.00372
3	QG80%	AS10%	GB10%	54.4	1.3	65.6	1.3	78.2	1.0	0.0271	0.00279
4	QG70%	AS30%	GB 0%	56.9	0.9	68.6	1.4	83.3	3.6	0.0306	0.00463
5	QG70%	AS15%	GB15%	59.9	1.3	71.5	1.5	86.7	3.9	0.0313	0.00628
6	QG60%	AS40%	GB 0%	65.5	1.4	76.6	2.7	95.2	4.3	0.0371	0.00339
7	QG60%	AS30%	GB10%	62.6	1.2	74.1	1.6	88.9	1.9	0.0339	0.00722
8	QG60%	AS20%	GB20%	59.8	1.3	71.9	1.1	90.4	4.0	0.0513	0.00917
9	QG60%	AS10%	GB30%	57.5	1.5	69.2	1.0	85.5	2.0	0.0478	0.00516
10	QG60%	AS0%	GB40%	52.1	0.6	63.2	1.0	77.5	0.8	0.0456	0.00297
11	QG50%	AS50%	GB 0%	73.9	1.9	87.3	2.4	104.5	3.7	0.0497	0.0108
12	QG50%	AS25%	GB25%	63.7	2.6	75.6	2.2	95.7	4.2	0.0615	0.00682
13	QG40%	AS60%	GB 0%	77.0	2.8	88.4	2.1	104.5	3.7	0.0464	0.00328
14	QG40%	AS30%	GB30%	66.7	1.0	80.9	1.6	106.2	3.2	0.0795	0.00778
15	QG0%	AS100%	GB 0%	95.8	1.7	113.2	2.6	136.2	2.4	0.117	0.00427

Table 1. Statistics on the means and standard deviations (S.D.) of the four characteristic quantities, X20, X50, X50, and Ps for total granular mass, under different compositions of quartz gravel (QG), angular stone (AS) and glass bead (GB).

Grain compositions in cases				X_{20} (cm)		X_{50} (cm)		X_{80} (cm)		P_s	
				Mean	S.D.	Mean	S.D.	Mean	S.D.	Mean	S.D.
1	QG100%	AS0%	GB 0%	NAN	NAN	NAN	NAN	NAN	NAN	NAN	NAN
2	QG80%	AS20%	GB 0%	63.7	3.3	76.7	3.9	96.0	7.2	0.0335	0.0127
3	QG80%	AS10%	GB10%	62.3	5.1	72.2	5.4	91.7	8.9	0.0442	0.0345
4	QG70%	AS30%	GB 0%	61.1	4.3	75.2	4.9	97.6	7.3	0.0471	0.0112
5	QG70%	AS15%	GB15%	66.5	3.9	78.4	7.4	98.1	9.9	0.0297	0.0277
6	QG60%	AS40%	GB 0%	71.9	3.0	83.5	4.3	103.5	5.2	0.0474	0.00568
7	QG60%	AS30%	GB10%	67.0	2.1	77.1	2.6	97.8	5.6	0.0385	0.0160
8	QG60%	AS20%	GB20%	67.5	3.3	80.9	6.5	108.8	11.2	0.0682	0.0285
9	QG60%	AS10%	GB30%	66.2	2.3	80.3	6.1	100.5	12.3	0.0715	0.0318
10	QG60%	AS0%	GB40%	NAN	NAN	NAN	NAN	NAN	NAN	NAN	NAN
11	QG50%	AS50%	GB 0%	79.2	2.8	91.2	4.6	111.0	6.9	0.0587	0.0230
12	QG50%	AS25%	GB25%	69.9	3.0	82.6	4.9	113.0	11.4	0.0837	0.0324
13	QG40%	AS60%	GB 0%	78.2	2.7	89.5	2.4	107.1	3.7	0.0493	0.00713
14	QG40%	AS30%	GB30%	75.2	2.9	92.2	3.0	118.2	7.9	0.0965	0.0245
15	QG0%	AS100%	GB 0%	95.8	1.7	113.2	2.6	136.2	2.4	0.117	0.00427

Table 2. Statistics on the means and standard deviations (S.D.) of the four characteristic quantities, X_{20}, X_{50}, X_{50}, and P_s for angular stone mass, under different compositions of quartz gravel (QG), angular stone (AS) and glass bead (GB). 'NAN' suggests there is no data obtained.

Cumulative frequency distributions among different cases

In general, experimentally obtained cumulative frequency distributions revealed that, as the fraction of angular stone increases, more materials (both total mass and angular stone mass) would be transported further (Figs. 5, 6, 7). However, such increase in granular mobility between two cases does not always occur throughout all node locations (except for both start node and end node). Sometimes, it occurs at short-distance locations; while sometimes it occurs at long-distance locations. For example, the cumulative frequencies in the case 6 (40%AS + 60%QG; the green line in Fig. 5a) at all locations are lower than those in the case 1 (0%AS + 100%QG; the red line in Fig. 5a), which suggests the increase of mobility at all locations; while the cumulative frequencies in the case 4 (30%AS + 70%QG; the dark green line in Fig. 5a) at the locations of larger than 80 cm are lower than those in the case 1 (0%AS + 100%QG; the red line in Fig. 5a), which suggests the increase of mobility only occurs at the locations of larger than 80 cm. It also could be easily found that the dispersion degree of original data points among five runs in each case for mass distributions of angular stone is higher than that for mass distributions of total mass (Comparing Figs. 5a, 6a, 7a with Fig. 5b, 6b, 7b). And, the high degree of dispersion typically occurs within the cumulative frequency range of 0.4–0.7 for both total mass and angular stone mass.

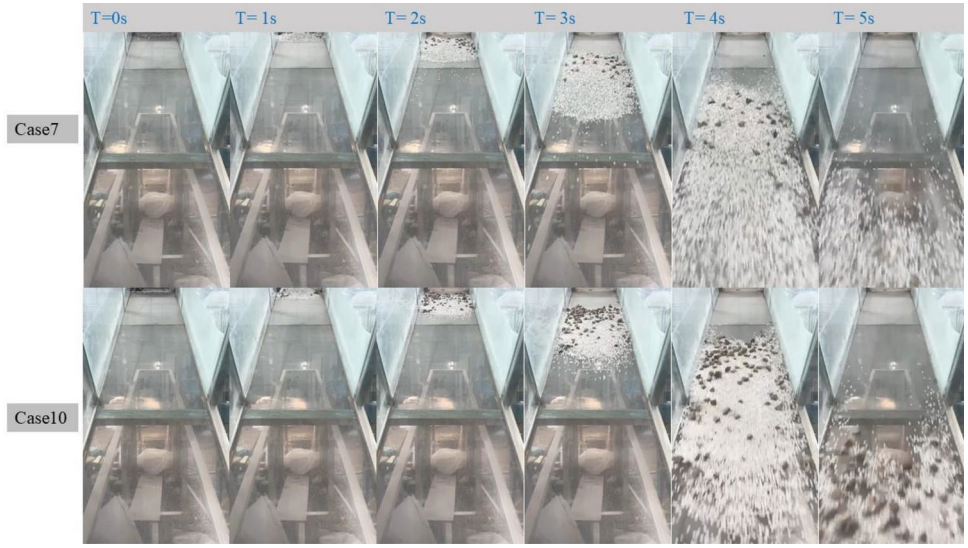

Fig. 4. The motion of granular particles along the chute of 2 cases of grain compositions for granular materials in terms of weight percentage (case7-QG 60%, AS 30%, GB 10% and case-10) QG 60%, AS 0%, GB 40%).

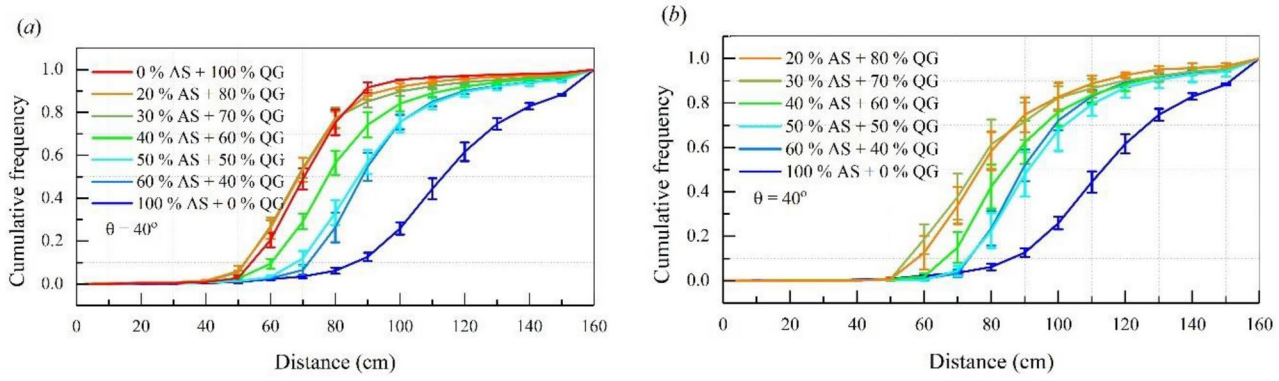

Fig. 5. Cumulative mass frequency of deposited granular materials versus horizontal distance responding to changes in the mass ratio of quartz gravel versus angular stone. (**a**) Total mass, (**b**) angular stone mass.

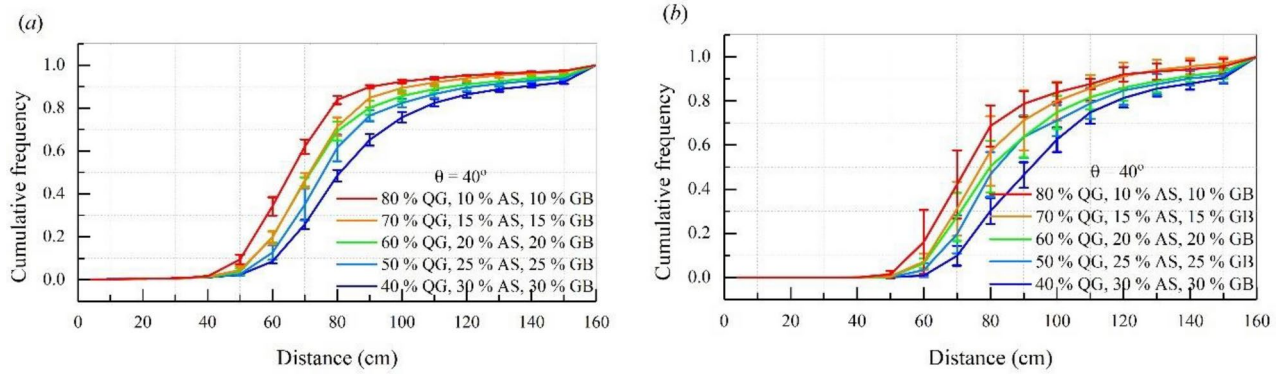

Fig. 6. Cumulative mass frequency of deposited granular materials versus horizontal distance responding to changes in the mass fraction of quartz gravel while angular stone mass: glass bead mass = 1:1. (**a**) Total mass, (**b**) angular stone mass.

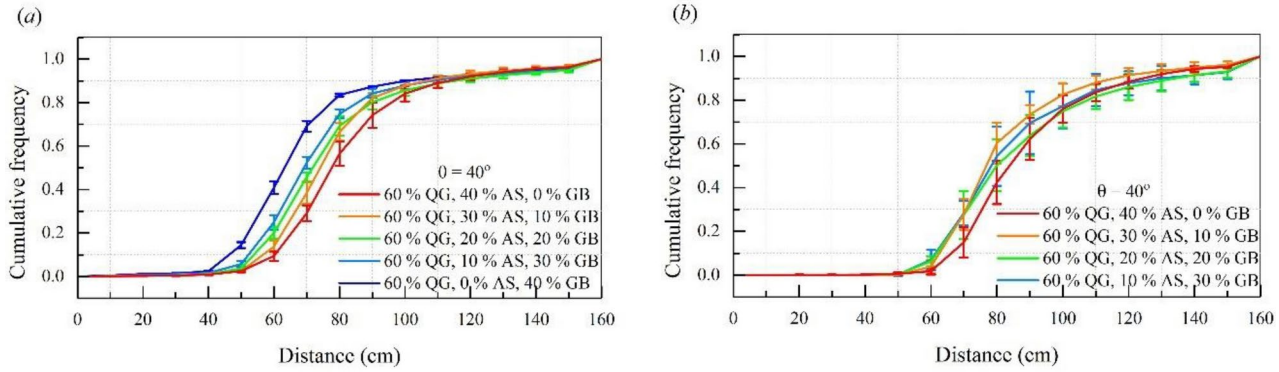

Fig. 7. Cumulative mass frequency of deposited granular materials versus horizontal distance responding to changes in the mass ratio of angular stone versus glass bead while keeping the mass fraction of quartz gravel. (**a**) Total mass, (**b**) angular stone mass.

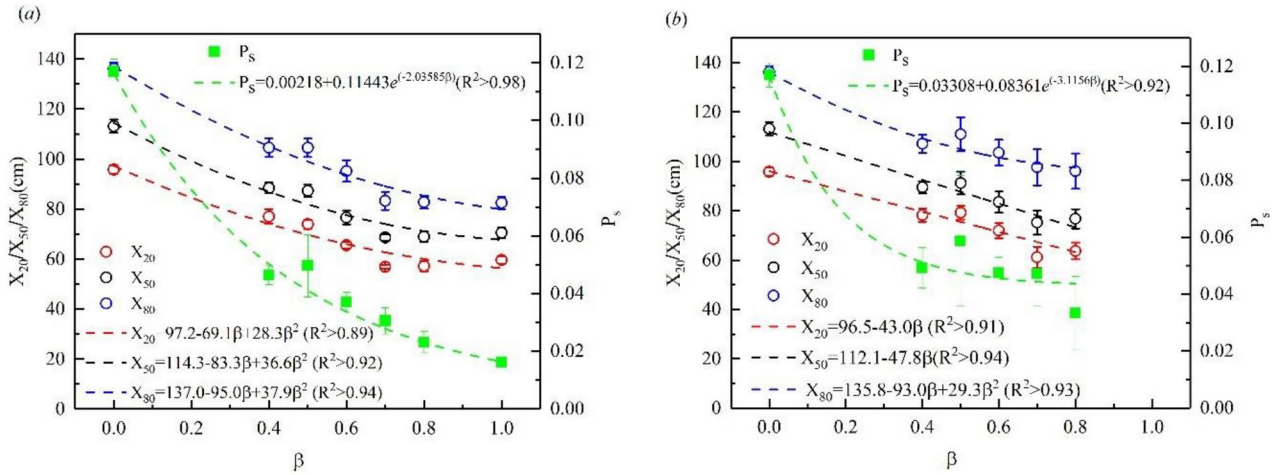

Fig. 8. X_{20}, X_{50} X_{80} and P_s versus β with cases 1, 2, 4, 6, 11, 13 and 15. (**a**) Total mass, (**b**) angular stone mass.

Characteristic quantities among different cases

By comparing with Tables 1 and 2, it could be found that the variations in both means and standard deviations (S.D.) of the four characteristic quantities, X_{20}, X_{50}, X_{80}, and P_s, responding to the change of grain compositions for total granular mass are qualitatively consistent with but still quantitatively different from those for angular stone mass. And, these differences vary with types of grain compositions.

To understand the role of angular stone on the mobility of granular materials, we choose cases 1, 2, 4, 6, 11, 13 and 15 for further analysis. We defined the fraction of quartz gravel as β (its value ranges from 0 to 1) in the following analysis. Figure 6 shows the X_{20}, X_{50} X_{80} and P_s versus β. This type of grain compositions, X_{20}, X_{50}, X_{80}, and P_s generally show an increase trend with the decrease of quartz gravel's fraction (or the increase of angular stone's fraction) (Table 1, Fig. 8). Further quantitative analyses reveal that they in fact increase differently with the decrease of quartz gravel's fraction. From Fig. 8, X_{20}, X_{50} and X_{80} are found to change with β in the parabolic form for total mass. The fitting curves for X_{20}, X_{50} and X_{80} are $X_{20}=97.2-69.1\beta+28.3\beta^2$ ($R^2>0.89$), $X_{50}=114.3-83.3\beta+36.6\beta^2$ ($R^2>0.92$), and $X_{80}=137.0-95.0\beta+37.9\beta^2$ ($R^2>0.94$), respectively. P_s is found to change with β in the exponential a form for total mass (Table 1, Fig. 8), i.e., $P_s=0.00218+0.11443\mathrm{Exp}(-2.03585\beta)$ ($R^2>0.98$). However, X_{20} and X_{50} are found to change with β in the linear form for angular stone mass (Table 2, Fig. 8). The detailed expressions are $X_{20}=96.5-43.0\beta$ ($R^2>0.91$) and $X_{50}=112.1-47.8\beta$ ($R^2>0.94$). X_{80} and P_s are found to change with β in the parabolic form and in the exponential form for angular stone mass (Table 2, Fig. 8), respectively. The detailed expressions are $X_{80}=135.8-73.0\beta+29.3\beta^2$ ($R^2>0.93$) and $P_s=0.03308+0.08361\mathrm{Exp}(-3.1156\beta)$ ($R^2>0.92$).

The role of grain shape on the mobility of granular materials also analyzed in this paper. We choose the type of grain compositions (cases 3, 5, 8, 12 and 14), to maintaining a 1:1 ratio of angular stone mass to glass bead mass. Figure 7 shows the X_{20}, X_{50} X_{80} and P_s versus β. The increase trends of X_{20}, X_{50}, X_{80}, and P_s with the decrease of quartz gravel's fraction (or the increase of angular stone's fraction) are still hold. However, X_{20}, X_{50}, X_{80}, and P_s are found to change with β in the linear form for total mass (Table 1, Fig. 9). The corresponding fitting curves are $X_{20}=78.0-28.5\beta$ ($R^2>0.91$), $X_{50}=93.9-34.6\beta$ ($R^2>0.92$), $X_{80}=130.5-65.0\beta$ ($R^2>0.96$),

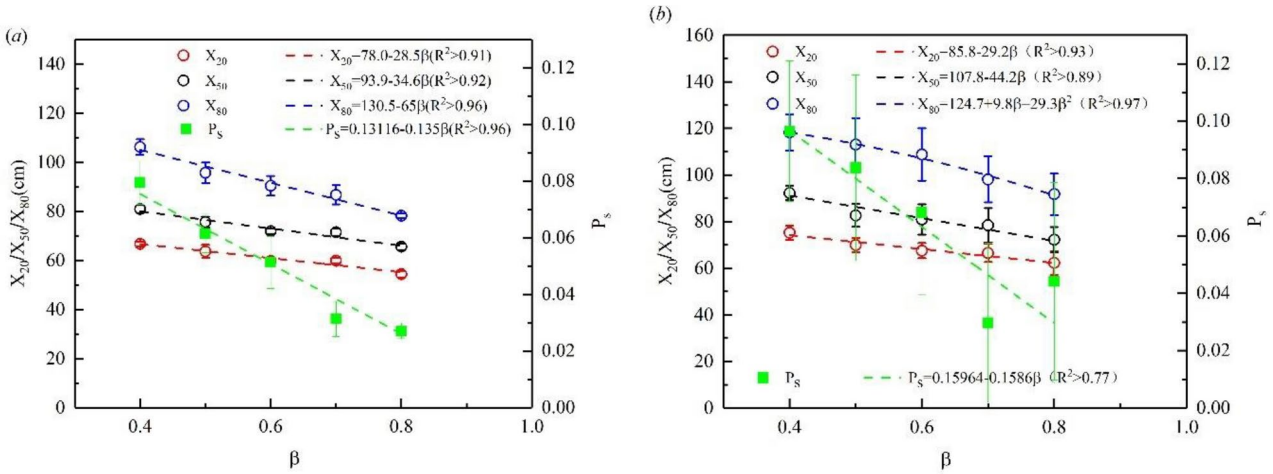

Fig. 9. X_{20}, X_{50} X_{80} and P_s versus β with cases 3, 5, 8, 12 and 14. (**a**) Total mass, (**b**) angular stone mass.

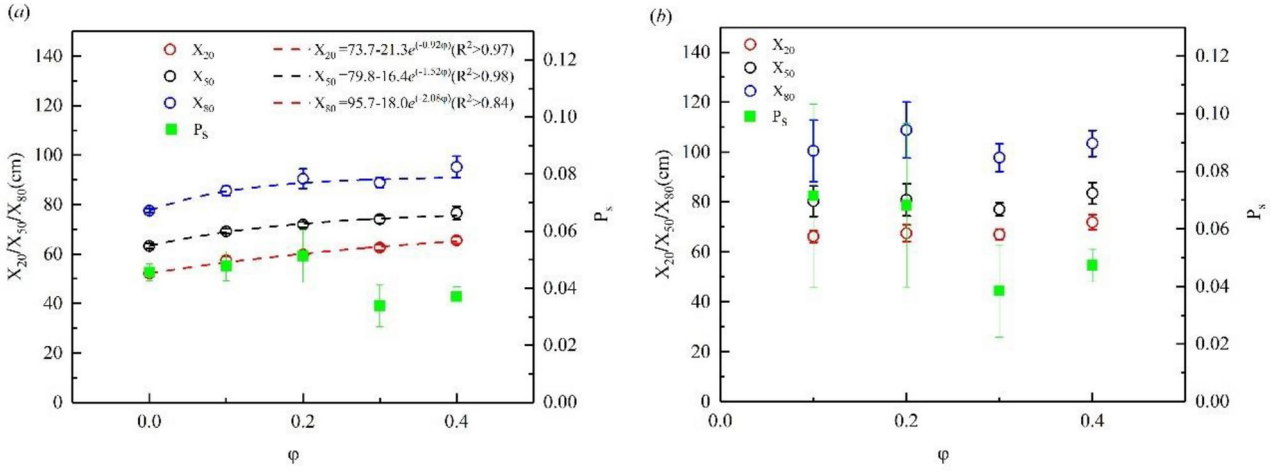

Fig. 10. X_{20}, X_{50} X_{80} and P_s versus φ with cases 6, 7, 8, 9 and 10. (**a**) Total mass, panel (**b**) angular stone mass.

and $P_s = 0.13116 - 0.135\beta$ ($R^2 > 0.96$). Bedsides, X_{20}, X_{50}, and P_s are found to change with β in the linear form for angular stone mass (Table 2, Fig. 9), but X_{80} is found to change with β in the parabolic form for angular stone mass. The corresponding fitting curves are $X_{20} = 85.8 - 29.2\beta$ ($R^2 > 0.93$), $X_{50} = 107.8–44.2\beta$ ($R^2 > 0.89$), $X_{80} = 124.7 + 9.8\beta - 29.3\beta^2$ ($R^2 > 0.97$), and $P_s = 0.15964 - 0.1586\beta$ ($R^2 > 0.77$).

As for the third type of grain compositions (cases 6, 7, 8, 9 and 10), the changes of X_{20}, X_{50}, X_{80}, and P_s with the increase of angular stone's fraction (or the decrease of glass bead's fraction) for total mass are different from those for angular stone mass. Here, let the angular stone's fraction in the mixture of angular stone and glass bead be denoted by φ, under the set of fixing quartz gravel's fraction, X_{20}, X_{50} and X_{80} are found to change with φ in the exponential form for total mass (Table 1, Fig. 10). The corresponding fitting curves are $X_{20} = 73.7 - 21.3\mathrm{Exp}(-0.92\varphi)$ ($R^2 > 0.97$), $X_{50} = 79.8 - 16.4\mathrm{Exp}(-1.52\varphi)$ ($R^2 > 0.98$), and $X_{80} = 95.7 - 18.0\mathrm{Exp}(-2.08\varphi)$ ($R^2 > 0.84$). But, X_{20}, X_{50} and X_{80} are found to be weakly related to φ for angular stone mass (Table 2, Fig. 10). Moreover, P_s exhibits high values at small φ and low values at large φ for both total mass and angular stone mass.

In fact, the inclusion of glass bead (correspondingly decreasing the fraction of angular stone by keeping the fraction of quartz gravel) in most of cases would decrease characteristic deposition distances (X_{20}, X_{50}, and X_{80}) for total mass (Table 1). However, the cases in which characteristic deposition distances increase with the inclusion of glass bead become frequent for angular stone mass (Table 2). For examples, X_{20}, X_{50}, and X_{80} for both total mass and angular stone mass in case 5 are higher than those in case 4; X_{80} for total mass in case 14 is higher than that in case 13, and X_{50} and X_{80} for stone mass in case 14 is higher than that in case 13. In contrast, including glass beads while maintaining a 1:1 ratio of angular stone mass to glass bead mass in most of cases leads to an increase in P_s. The decrease of P_s only occurs at the situation that the fraction of quartz gravel mass keeps at 70% (case 4 vs case 5).

Furthermore, two main points could be found from the variations in S.D.s. The first point is that the averaged value of S.D.s among different characteristic deposition distances is in proper order: X_{20}, X_{50}, and X_{80}. And, the

averaged S.D.s for angular stone mass (X_{20}: 3.1 cm, X_{50}: 4.5 cm, and X_{80}: 7.7 cm) are higher than those for total mass (X_{20}: 1.6 cm, X_{50}: 1.8 cm, and X_{80}: 3.1 cm). The second one is that the coefficients of variation for P_s (ranging from 0.036 to 0.445) are typically higher than those for X_{20}, X_{50}, and X_{80} (ranging from 0.010 to 0.122). Besides, it could be found that coefficients of variation for angular stone mass are larger than those for total mass.

Discussion and conclusions

This piece of work conducted laboratory experiments to measure the mass frequency distributions of granular materials in different grain compositions. Based on our experimental design, granular materials experienced three stages (slide along slope, free fall, and movement on flat bed surface) before final deposit. As mentioned above, roads were sometimes located at the foot of hills at mountain areas. To utilize the convenience brought by roads, human beings nearby would like to construct buildings for living purpose or flat ground for commercial purpose (e.g., parking) at the roads' side opposite to hills. Besides, granular materials on the slope of open pit during blasting or other operations[43,44] may experience similar three movement stages. Therefore, our investigations here could be helpful for assessing and reduce the disaster risk induced by granular flows from mountain top.

Four characteristic quantities (three distances and one probability) were extracted from cumulative frequency distributions of deposited mass. Results obtained here demonstrated again the importance of large grain on the mobility of the whole mixture[15,27], which also may be influenced by grain size ratio (the ratio of large grain versus small grain), grain density, grain shape and grain composition. Previous study[45] showed that the mobility (represented by horizontal distance) of mixture at grain size ratio = 4 would increase with the fraction of large grains and then decrease after reaching a maximum value, which is different with our results (grain size ratio in our experiments is about 4 as shown above). In our experiments, the change of grain densities is relatively small, which suggests the effects of grain densities could be neglected. Therefore, the main reason for the difference might be grain shape. In the previous study circular grains were used for both large and small grains, while in our study angular grains were used for both large and small grains.

However, as for total mass, characteristic deposition distances (X_{20}, X_{50}, and X_{80}) decreased and extreme mobility probability (P_s) increased in most of cases when including glass bead; and, as for angular stone mass, the cases in which X_{20}, X_{50}, and X_{80} increase with the inclusion of glass bead become frequent apart from that P_s increased in most of cases. These results indicate two main aspects. The first aspect is that small round grains could effectively enhance the extreme mobility of large angular stones, even if the mass fraction of angular stone is reduced. The second one is that, in the mixture of three kinds of grains, the mobility of small angular grains (size similar to small round grains) could be partially limited. In view of the low lose rate of energy during collisions with similar size angular grains and the low friction coefficient, the effect of including glass bead may be explained as follows. For dry granular flows, small round grains are much easier to fall into the spaces (or voids) formed between large angular stones and small angular grains near bed[6]. Thus, small round grains could act as resistance for small angular grains and assistance for large angular stones. For example, round grains obtain energy through grain-grain collisions with small angular grains (this process typically reduces the motion of small angular grains) and then travel to upper layer of grain flows and collide with large angular stones (this process may increase the motion of large angular stones). In conclude, small round grains reduce the effective friction of bed surface for large angular stones through grain-grain and grain-bed interaction[26]. Nevertheless, this mechanism could not explain all results in this work. More well-designed experiments are required to interpret the uncommon results in the future.

Data availability

All data generated or analyzed during this study are included in this published article. Data is provided within the supplementary information files.

Received: 4 July 2024; Accepted: 18 November 2024
Published online: 27 November 2024

References

1. Zheng, X. *Mechanics of Wind-Blown Sand Movements* (Springer, 2009).
2. Yin, Y., Wang, F. & Sun, P. Landslide hazards triggered by the 2008 Wenchuan earthquake, Sichuan, China. *Landslides* **6**(2), 139–152. https://doi.org/10.1007/s10346-009-0148-5 (2009).
3. Delannay, R., Valance, A., Mangeney, A., Roche, O. & Richard, P. Granular and particle-laden flows: From laboratory experiments to field observations. *J. Phys. D Appl. Phys.* **50**(5), 053001. https://doi.org/10.1088/1361-6463/50/5/053001 (2017).
4. Jian, F., Narendran, R. B. & Jayas, D. S. Segregation in stored grain bulks: Kinematics, dynamics, mechanisms, and minimization—A review. *J. Stored Prod. Res.* **81**, 11–21. https://doi.org/10.1016/j.jspr.2018.12.004 (2019).
5. Makse, H. A. Grain segregation mechanism in aeolian sand ripples. *Eur. Phys. J. E* **1**(2), 127–135. https://doi.org/10.1007/PL00014592 (2000).
6. Vallance, J. W. & Savage, S. B. Particle segregation in granular flows down chutes. In *IUTAM Symposium on Segregation in Granular Flows* (eds Rosato, A. D. & Blackmore, D. L.) 31–51 (Springer, 2000).
7. Gray, J. M. N. T. & Chugunov, V. A. Particle-size segregation and diffusive remixing in shallow granular avalanches. *J. Fluid Mech.* **569**, 365–398. https://doi.org/10.1017/S0022112006002977 (2006).
8. Zhou, G. D., Sun, Q. C. & Cui, P. Study on the mechanisms of solids segregation in granular debris flows. *J. Sichuan Univ. Ed.* **45**, 28 (2013).
9. Takahashi, T. Debris flow. *Annu. Rev. Fluid Mech.* **13**(1), 57–77. https://doi.org/10.1146/annurev.fl.13.010181.000421 (1981).
10. Gray, J. M. N. T., Tai, Y. C. & Hutter, K. Shock waves and particle size segregation in shallow granular flows. In *IUTAM Symposium on Segregation in Granular Flows* (eds Rosato, A. D. & Blackmore, D. L.) 269–276 (Springer, 2000).
11. Crosta, G. B., Frattini, P. & Fusi, N. Fragmentation in the Val Pola rock avalanche, Italian Alps. *J. Geophys. Res.* **112**, F01006. https://doi.org/10.1029/2005JF000455 (2007).

12. Gray, J. M. N. T. Particle segregation in dense granular flows. *Annu. Rev. Fluid Mech.* **50**, 407–433. https://doi.org/10.1146/annurev-fluid-122316-045201 (2018).
13. Sheng, L. T., Hsiau, S. S. & Hsu, N. W. Experimental study of the dynamic behavior and segregation of density-bidisperse granular sliding masses at the laboratory scale. *Landslides* **18**(6), 2095–2110. https://doi.org/10.1007/s10346-021-01629-1 (2021).
14. Wang, C., Cui, Y., Song, D., Nie, J. & Hu, B. Effect of ice content on the interaction between rock–ice avalanche and rigid barrier: Physical and numerical modelling. *Comput. Geotech.* **150**, 104924. https://doi.org/10.1016/j.compgeo.2022.104924 (2022).
15. Phillips, J. C., Hogg, A. J., Kerswell, R. R. & Thomas, N. H. Enhanced mobility of granular mixtures of fine and coarse particles. *Earth Planet. Sci. Lett.* **246**(3–4), 466–480. https://doi.org/10.1016/j.epsl.2006.04.007 (2006).
16. Wiederseiner, S. et al. Experimental investigation into segregating granular flows down chutes. *Phys. Fluids* **23**(1), 013301. https://doi.org/10.1063/1.3536658 (2011).
17. Johnson, C. G. et al. Grain-size segregation and levee formation in geophysical mass flows. *J. Geophys. Res. Earth* **117**(F1), F01032. https://doi.org/10.1029/2011JF002185 (2012).
18. van der Vaart, K. et al. Underlying asymmetry within particle size segregation. *Phys. Rev. Lett.* **114**(23), 238001. https://doi.org/10.1103/PhysRevLett.114.238001 (2015).
19. Frey, P. et al. Experiments on grain size segregation in bedload transport on a steep slope. *Adv. Water Resour.* **136**, 103478. https://doi.org/10.1016/j.advwatres.2019.103478 (2020).
20. Hotta, N., Iwata, T., Suzuki, T. & Sakai, Y. The effects of particle segregation on debris flow fluidity over a rigid bed. *Environ. Eng. Geosci.* **27**(1), 139–149. https://doi.org/10.2113/EEG-D-20-00106 (2021).
21. Trewhela, T., Ancey, C. & Gray, J. M. N. T. An experimental scaling law for particle-size segregation in dense granular flows. *J. Fluid Mech.* **916**, A55. https://doi.org/10.1017/jfm.2021.227 (2021).
22. Sharp, R. P. & Nobles, L. H. Mudflow of 1941 at Wrightwood, southern California. *Geol. Soc. Am. Bull.* **64**(5), 547–560. https://doi.org/10.1130/0016-7606(1953)64[547:MOAWSC]2.0.CO;2 (1953).
23. Zhang, L. M., Xu, Y., Huang, R. Q. & Chang, D. S. Particle flow and segregation in a giant landslide event triggered by the 2008 Wenchuan earthquake, Sichuan, China. *Nat. Hazards Earth Syst. Sci.* **11**(4), 1153–1162. https://doi.org/10.5194/nhess-11-1153-2011 (2011).
24. Marc, O., Turowski, J. M. & Meunier, P. Controls on the grain size distribution of landslides in Taiwan: The influence of drop height, scar depth and bedrock strength. *Earth Surf. Dynam.* **9**(4), 995–1011. https://doi.org/10.5194/esurf-9-995-2021 (2021).
25. Jing, L., Kwok, C. Y. & Leung, Y. F. Micromechanical origin of particle size segregation. *Phys. Rev. Lett.* **118**(11), 118001. https://doi.org/10.1103/PhysRevLett.118.118001 (2017).
26. Chassagne, R., Frey, P., Maurin, R. & Chauchat, J. Mobility of bidisperse mixtures during bedload transport. *Phys. Rev. Fluids* **5**(11), 114307. https://doi.org/10.1103/PhysRevFluids.5.114307 (2020).
27. Fan, X. Y., Tian, S. J. & Zhang, Y. Y. Mass-front velocity of dry granular flows influenced by the angle of the slope to the runout plane and particle size gradation. *J. Mt. Sci.* **13**(2), 234–245. https://doi.org/10.1007/s11629-014-3396-3 (2016).
28. Tripathi, A. & Khakhar, D. V. Rheology of binary granular mixtures in the dense flow gime. *Phys. Fluids* **23**(11), 147–252. https://doi.org/10.1063/1.3653276 (2011).
29. Barker, T. et al. Coupling rheology and segregation in granular flows. *J. Fluid Mech.* https://doi.org/10.1017/JFM.2020.973 (2021).
30. Deng, T., Garg, V., Salehi, H. & Bradley, M. S. An experimental study on free-surface rolling segregation and correlations with angle of repose and particle sphericity. *Powder Technol.* **379**, 307–320. https://doi.org/10.1016/j.powtec.2020.10.077 (2021).
31. Dai, B. B. et al. Particle sorting in scree slopes: Characterization and interpretation from the micromechanical perspective. *J. Geophys. Res. Earth* **127**, e2021JF006372. https://doi.org/10.1029/2021JF006372 (2022).
32. Ge, Y. et al. Deposit characteristics of the Jiweishan rapid long-runout landslide based on field investigation and numerical modeling. *Bull. Eng. Geol. Environ.* **78**(6), 4383–4396. https://doi.org/10.1007/s10064-018-1422-3 (2019).
33. Perinotto, H. et al. The extreme mobility of debris avalanches: A new model of transport mechanism. *J. Geophys. Res Sol. Earth* **120**(12), 8110–8119. https://doi.org/10.1002/2015JB011994 (2015).
34. Zhao, W., Wang, R., Liu, X., Ju, N. & Xie, M. Field survey of a catastrophic high-speed long-runout landslide in Jichang Town, Shuicheng County, Guizhou, China, on July 23, 2019. *Landslides* **17**(6), 1415–1427. https://doi.org/10.1007/s10346-020-01380-z (2020).
35. Zhou, W., Lai, Z., Ma, G., Yang, L. & Chen, Y. Effect of base roughness on size segregation in dry granular flows. *Granular Matter* **18**, 1–14. https://doi.org/10.1007/s10035-016-0680-7 (2016).
36. Li, S., Chen, X., Zhou, G., Song, D. & Chen, J. (2018). Influence of bulk density and slope on debris flows deposit morphology: Physical modelling. In *Proceedings of China-Europe Conference on Geotechnical Engineering*, vol. 2, 1495–1499 (Springer, 2018).
37. Jiang, Y. J., Fan, X. Y., Li, T. H. & Xiao, S. Y. Influence of particle-size segregation on the impact of dry granular flow. *Powder Technol.* **340**, 39–51. https://doi.org/10.1016/j.powtec.2018.09.014 (2018).
38. Zhou, Y. et al. 3D DEM investigation on the morphology and structure of landslide dams formed by dry granular flows. *Eng. Geol.* **258**, 105151. https://doi.org/10.1016/j.enggeo.2019.105151 (2019).
39. Hu, Y. X., Li, H. B., Qi, S. C., Fan, G. & Zhou, J. W. Granular effects on depositional processes of debris avalanches. *KSCE J. Civ. Eng.* **24**(4), 1116–1127. https://doi.org/10.1007/s12205-020-1555-3 (2020).
40. Hu, Y. X., Li, H. B., Lu, G. D., Fan, G. & Zhou, J. W. Influence of size gradation on particle separation and the motion behaviors of debris avalanches. *Landslides* **18**, 1845–1858. https://doi.org/10.1007/s10346-020-01596-z (2021).
41. Wu, Y. B., Duan, Z., Peng, J. B., Zhang, Q. & Pähtz, T. Influence of slope angle on deposit morphology and propagation of laboratory landslides. *Sci. Rep.* **13**(1), 9452. https://doi.org/10.1038/s41598-023-36554-x (2023).
42. May, R. A. & Stevenson, K. J. Software review of Origin 8. *J. Am. Chem. Soc.* **131**(2), 872–872. https://doi.org/10.1021/ja809638x (2009).
43. Su, H. & Ma, S. Study on the stability of high and steep slopes under deep bench blasting vibration in open-pit mines. *Front. Earth Sci.* **10**, 990012. https://doi.org/10.3389/feart.2022.990012 (2022).
44. Zhang, J. et al. Numerical and theoretical investigations of the effect of the gangue-coal density ratio on the drawing mechanism in longwall top-coal caving. *Int. J. Coal Sci. Technol.* **9**(1), 1–20. https://doi.org/10.1007/s40789-022-00501-4 (2022).
45. Linares-Guerrero, E., Goujon, C. & Zenit, R. Increased mobility of bidisperse granular avalanches. *J. Fluid Mech.* **593**, 475–504. https://doi.org/10.1017/S0022112007008932 (2007).

Acknowledgements

The research reported in this manuscript is funded by the National Key Research and Development Program of China (2023YFC3006704), the Special Project for the Construction of Nyingchi National Sustainable Development Pilot Zone (2023-SYQ-006), the Second Tibetan Plateau Scientific Expedition and Research (No. 2019QZKK0903-2), the High-Level Talent Training Program in Chengdu University (Number 2081921086), the Sichuan Province Natural Science Foundation Project (Number 2023NSFSC0384), the Nyingchi National Sustainable Development Experimental Zone Project (2023-SYQ-007) and the Science and Technology Research Program of Institute of Mountain Hazards and Environment, Chinese Academy of Sciences (Grant No. IMHE-ZDRW-02).

Author contributions

Hai-Hua Gu and Lin-Tao Fu conducted the experiment(s). Hai-Hua Gu, Lin-Tao Fu and Yu Lei performed statistical analysis, figure generation, Writing and editing. All authors reviewed the manuscript.

Declarations

Competing interests

The authors declare no competing interests.

Additional information

Supplementary Information The online version contains supplementary material available at https://doi.org/10.1038/s41598-024-80361-x.

Correspondence and requests for materials should be addressed to H.-H.G.

Reprints and permissions information is available at www.nature.com/reprints.

Publisher's note Springer Nature remains neutral with regard to jurisdictional claims in published maps and institutional affiliations.